Centro de Astrofísica da Universidade do Porto

Universidade de Lisboa, SIM/IDL & LOLS

INAF, Osservatorio Astronomico di Trieste

INAF, Osservatorio Astronomico di Brera

Observatory of the University of Geneva

ESPRESSO

Fabry-Pérot Calibrator

Test Report

VLT-TRE-ESP-13520-9202, Issue 1

May 4th, 2016

Prepared	F. Pepe	4/05/2016	
	Name	Date	Signature
Approved	F. Zerbi		
	Name	Date	Signature
Released	F. Pepe		
	Name	Date	Signature

Change Record

Issue/Rev.	Date	Section/Page affected	Reason/Remarks
1	04/05/2016	All	Prepared in view of Sub-system acceptance

Table of Contents

List of Figures

List of Tables

Chapter 1. Introduction

1.1 Scope of the Document

This document describes the tests on the Fabry-Pérot Calibrator (FPC) performed in order to demonstrate compliance with sub-system requirements. For the detailed design description we refer to RD-2.

1.2 Documents

The applicable and reference documents are listed below:

1.2.1 Applicable Documents

AD-1	ESPRESSO Statement of Work	VLT-SOW-ESO-13520-5059	1	01.02.2011
AD-2	ESPRESSO Technical Specifications	VLT-SPE-ESO-13520-4633	3	01.02.2011

1.2.2 Reference Documents

RD-1	Fabry-Pérot Calibrator Final Design Description and Performances Analysis	VLT-TRE-ESP-13520-0154	2	04.05.2016
RD-2	Fabry-Pérot Calibrator Product Tree	VLT-LIS-ESP-13520-9201	1	04.05.2016

1.3 Acronyms and Abbreviations

1.3.1 Acronyms

AD	Applicable Document
AIV	Assembly, Integration and Verification
CCL	Combined Coudé Laboratory (of the VLT)
CIDL	Configuration Items Data List
CTE	Coefficient of Thermal Expansion
E-ELT	European Extremely Large Telescope
ESO	European Southern Observatory
ESPRESSO	Echelle Spectrograph for Rocky Exoplanets and Stable Spectroscopic Observations
FDR	Final Design Review
FP	Fabry-Pérot (etalon)
FPC	Fabry-Pérot Calibrator
FWHM	Full-Width at Half Maximum
HW	Hardware
ICD	Interface Control Document
ICS	Instrument Control Software
ISO	International Organisation for Standardisation
IP	Instrumental Profile

LDLS	Laser-Driven Light Source
LFC	Laser-Frequency Comb
LRU	Line-Replaceable Unit
MTBF	Mean Time Between Failures
N/A	Not Applicable
PAC	Provisional Acceptance Chile
PAE	Provisional Acceptance Europe
PDR	Preliminary Design Review
PI	Principal Investigator
PLC	Programmable Logic Controller
PM	Project Manager
QA	Quality Assurance
RAMS	Reliability Availability Maintainability Safety
RD	Reference Document
RfW	Request for Waiver
RV	Radial Velocity
SOW	Statement Of Work
SW	Software
TBC	To Be Confirmed
TBD	To Be Defined/To Be Developed
ThAr	Thorium-Argon (lamp)
ULE	Ultra-Low Expansion (material)
UPS	Uninterrupted Power Supply
UT	Unit Telescope (8.2 meter telescope at Paranal)
VLT	Very Large Telescope
VM	Verification Matrix
WBS	Work Breakdown Structure
WP	Work Package

Chapter 2. Verification Matrix

In the following Table 1 we recall the subsystem requirements for the FPC defined in RD-2 and propose a verification method.

Table 1: FPC Requirements and Verification Matrix

Item	Requirement	Verification DATSI + Comment
Wavelength coverage	380 – 780 nm	S: HARPS-N, T: At system level with ESPRESSO
System transmittance	> 10% In the wavelength range	T: At various wavelength, in lab.
Transmittance uniformity	$T_{max}/T_{min} < 2$ In the wavelength range	T: At various wavelength, in lab..
Transmittance variations	$dT/d\lambda < 2\%$ per nm	S: HARPS-N, T: At system level with ESPRESSO
Etalon total Finesse	$10 < F_E < 12$ In the wavelength range	T: HeNe laser, Pressure scan in lab.
Etalon spacing	$D = 7.6$ mm $\pm$ 0.0005 mm	D, T: Manufacturer of Etalon
Photon noise	< 5 cm/s Global precision achieved in a single exposure	S: HARPS-N, T: At system level with ESPRESSO
Flux homogeneity	$F_{max}/F_{min} < 5$ In the wavelength range	S: HARPS-N, T: At system level with ESPRESSO
Line width	$\delta\lambda <$ 2/3 of spectral element A spectral element is the wavelength divided by the spectral resolution	T: HeNe laser, Pressure scan in lab
Line separation	$\Delta\lambda$=2-7 x spectral element	T: HeNe laser, Pressure scan in lab
Short-term repeatability	$d\lambda/dt < 2\ 10^{-10}\ \lambda$(0.07 m/s) Over 12 hours	S: HARPS, T: At system level with ESPRESSO
Long-term repeatability and line-shape stability	$d\lambda/dt < 2\ 10^{-10}\ \lambda$(0.07 m/s) Over 20 years (goal)	S: HARPS, T: At system level with ESPRESSO
Local wavelength accuracy	$\lambda - \lambda_0 < 3 \times 10^{-8} \lambda$ (10 m/s) For any FPC line with respect to theoretical	S: HARPS, T: At system level with ESPRESSO

Chapter 3. Performance Verification

In the following we shall present the results obtained with ESPRESSO's FPC. Some parameters could not be verified in laboratory due to the absence of a highly stable high-resolution spectrograph. In those cases the performances is demonstrated by similarity with the performances of the HARPS and HARPS-N Fabry-Pérots. It must be pointed out that ESPRESSO FPC design is an exact copy of HARPS-N's Fabry-Pérot system.

3.1 Wavelength coverage and energy distribution

The high-resolution spectrum of the FPC system of the HARPS spectrograph is shown in Figure 1. Only a part of the raw frame is shown, as the whole image would be too large and the various lines would not be resolved individually. One can see the spectra of the two fibers both illuminated by the FPC system spectrum. The wavelength increases from left to right and from bottom to top, direction over which the spectrum is split over several echelle orders. The large gap in the center of the image is due to a physical gap in the CCD mosaic composed of two CCDs. For comparison a frame is shown in which one of the fiber was illuminated with the thorium lamp. Note the richness of the FP spectrum compared to that of the thorium!

Figure 1: Top: Raw HARPS frame of the FPC spectrum illuminating both fibers. Bottom: For comparison, a frame is shown in which one of the fiber was illuminated with the thorium lamp. Note the richness of the FPC spectrum compared to that of the thorium.

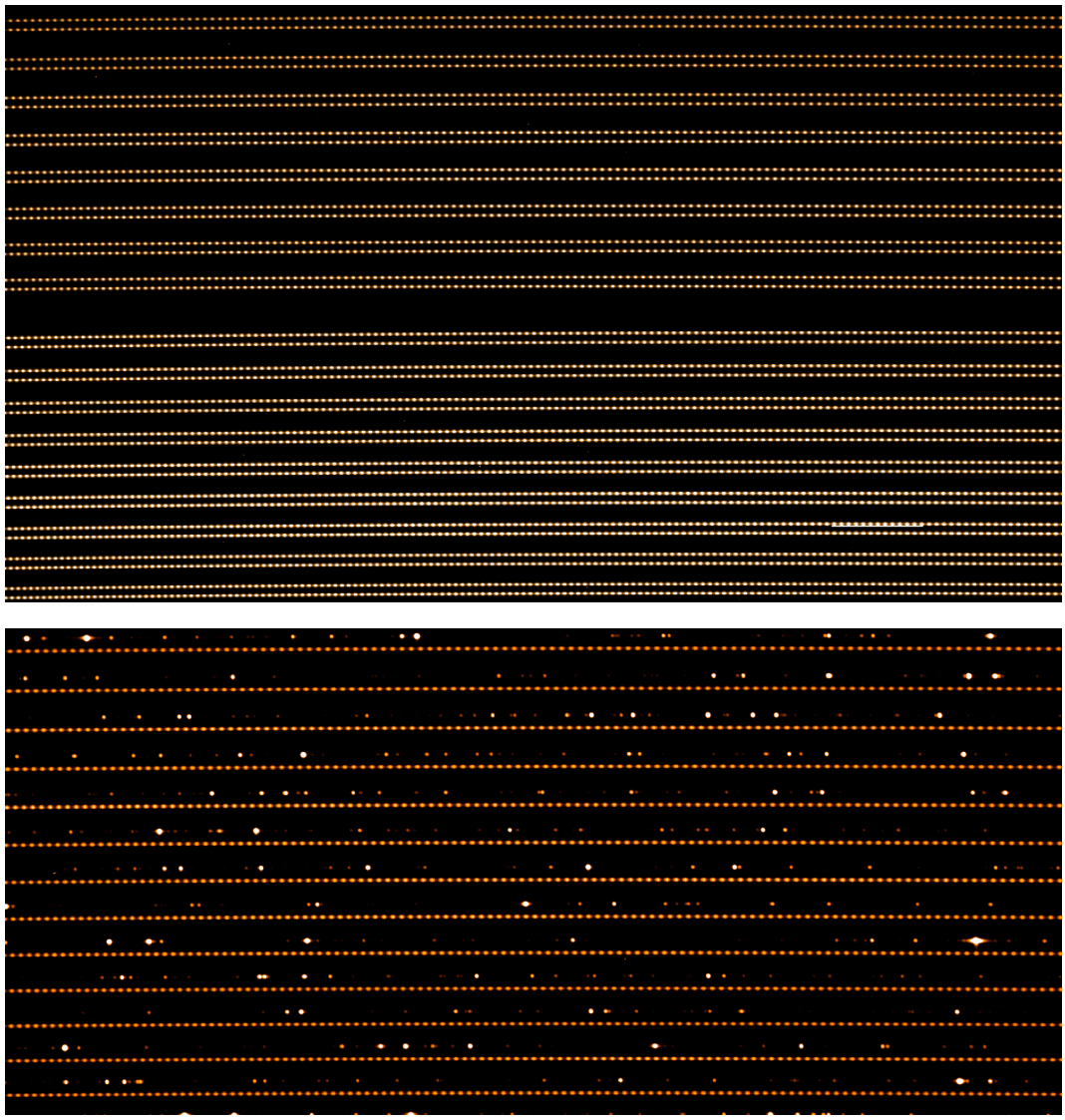

The average transmission of the FPC system has been measured using a low-resolution spectrograph. The reference spectrum was recorded by injecting the light of a tungsten lamp into a 200 μm fiber, in turn connected to a 600 μm fiber injecting the light into the spectrometer. The FPC spectrum was then recorded by separating the two fiber section and connecting the 200 μm fiber to the 200 μm input fiber port of the FPC and the 600 μm fiber to the 600 μm fiber output port of the FPC. The transmittance spectrum was determined by deviding the FPC spectrum by the reference spectrum after having subtracted the dark spectra.

Figure 2: Left: Transmission spectrum of the Fabry-Pérot etalon averaged of a broad band (>> than a typical FSR of the etalon). Right: flux at the peak of a transmission line of the FP when illuminated by the Xe-lamp compared to the tungsten lamp. Measurements have been carried out with HARPS.

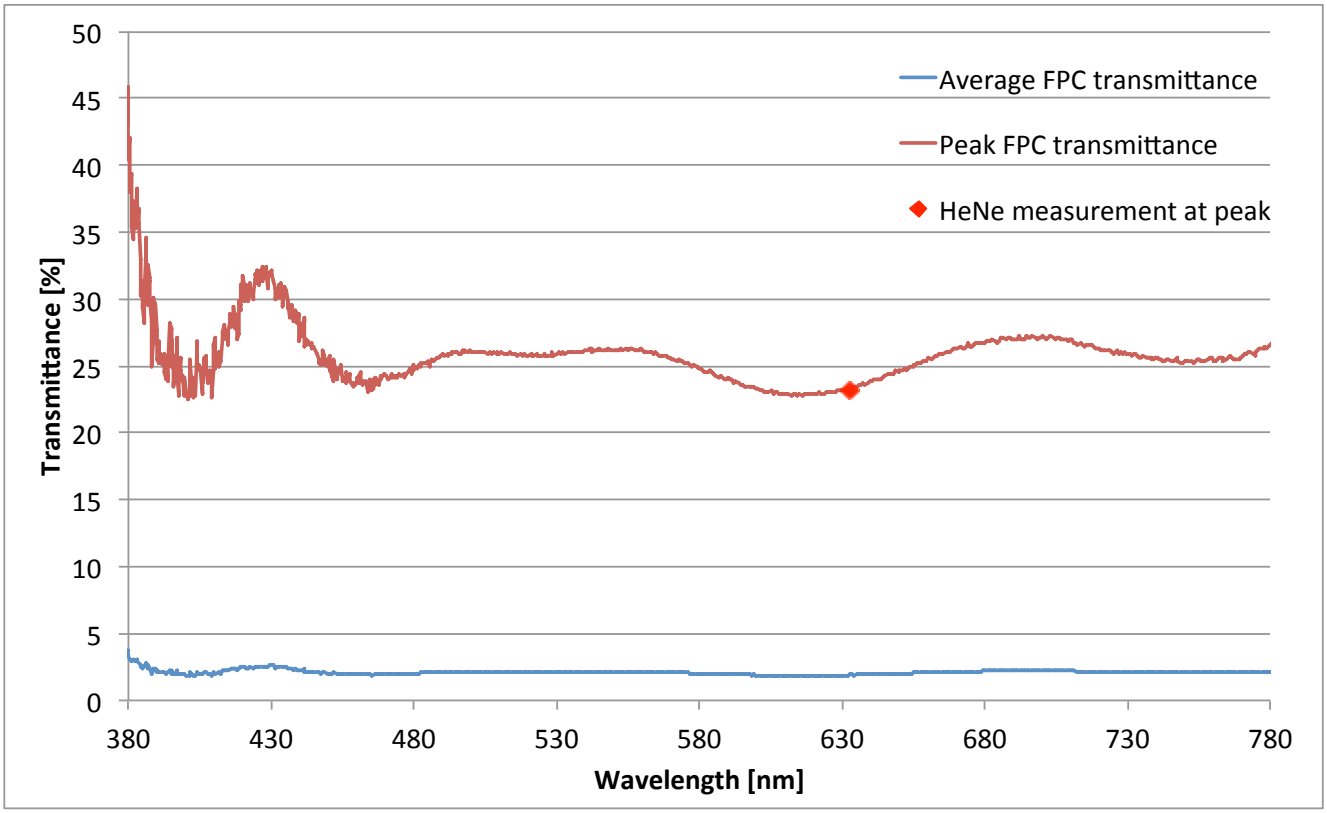

The resulting transmission spectrum is shown by the blue line in Figure 2. The spectrum shows however only an 'average' transmittance of the FPC given the low resolution of the spectrograph, which cannot resolve individual FPC lines. In order to determine the transmission at peak this value has to be multiplied by the Finesse of the etalon. As we will see later, the finesse measured is 12.27. The resulting peak-transmittance is shown by the red curve.

Although the blue part of the spectrum is affected by some measurement noise, mainly shot noise, it can be clearly seen that **the FPC covers the whole spectral range of ESPRESSO**. This is also by the spectra recorded with HARPS-N, of which the FPC has been in operation for more than 3 years.

3.2 System Transmittance

As seen in Figure 2 the system **transmittance lies everywhere between 22% and 40%,** and is thus significantly larger than the required minimum $\boldsymbol{T > 10\%}$. An independent verification of the absolute transmittance has been made by feeding the FPC with an HeNe laser and repeating the reference and FPC measurement described above while using a radiometer. In order to obtain peak transmittance to be compared with the read curve in Figure 2, we have scanned the pressure inside the FPC to obtain maximum transmittance. The result, indicated by the red diamond at 632.8 nm, is perfectly in line with the transmission spectrum.

3.3 Transmittance Uniformity

The maximum transmittance $T_{\max}$ is reached at the very blue end of the spectrum and is about 40%, while $T_{\min}$ is about 22%. Therefor the transmittance uniformity $\boldsymbol{T_{\max}/T_{\min} = 1.82 < 2}$ just in line with the specified requirement.

3.4 Transmittance Variations

The maximum transmittance variation $\mathrm{d}T/\mathrm{d}\lambda$ is observed between 380 and 400 nm dropping from 40% to 25% within 20nm. We compute then a relative flux variation of the order 37%, which produces a slope of $\boldsymbol{\mathrm{d}T/\mathrm{d}\lambda = 1.85\%/nm}$.

3.5 Finesse and Spectral Resolution

The finesse $F = \Delta\lambda/\delta\lambda$ (distance of two neighboring lines divided by the line width of a line) of the FP etalon has been measured in laboratory by scanning the etalon's effective gap. The scanning was achieved by varying the pressure inside the vacuum vessel and consequently between the two mirrors of the etalon. Thus, an effective optical path difference (OPD) is introduced and the transmitted wavelength changed. A commercial HeNe laser of λ = 632.8 nm was used for the line scanning measurement.

Figure 3 shows the transmitted laser flux as a function of effective optical gap variation as computed assuming a linear relationship between pressure and refractive index of air. The red curve corresponds to the Airy function which theoretically describes the transmittance function of the FP etalon with a single effective finesse F_E. The measured F_E is in our case simply the ratio between the FWHM of a single peak divided by the distance between two neighboring peaks, or can be determined by fitting an Airy function with F_E as one of the free parameters. In both cases we ontain a finesse $\boldsymbol{F_E = 12.27}$. This value corresponds exactly to the designed and thus expected value, and is therefor perfectly compliant with the minimum requirement of F_E = 12.27. Although is lies slightly outside the higher end on the specified range, we have to mention that a) the measurement of the finesse can be affected by small measurement errors and b) the higher finesse only impacts the flux delivered by the FPC, we may be reduced by a couple of percents. We consider therefore the FPC to be fully compliant with the finesse requirement.

Figure 3: Direct measurement of the FP transmittance when varying the optical length of the gap by varying the pressure inside the FPC

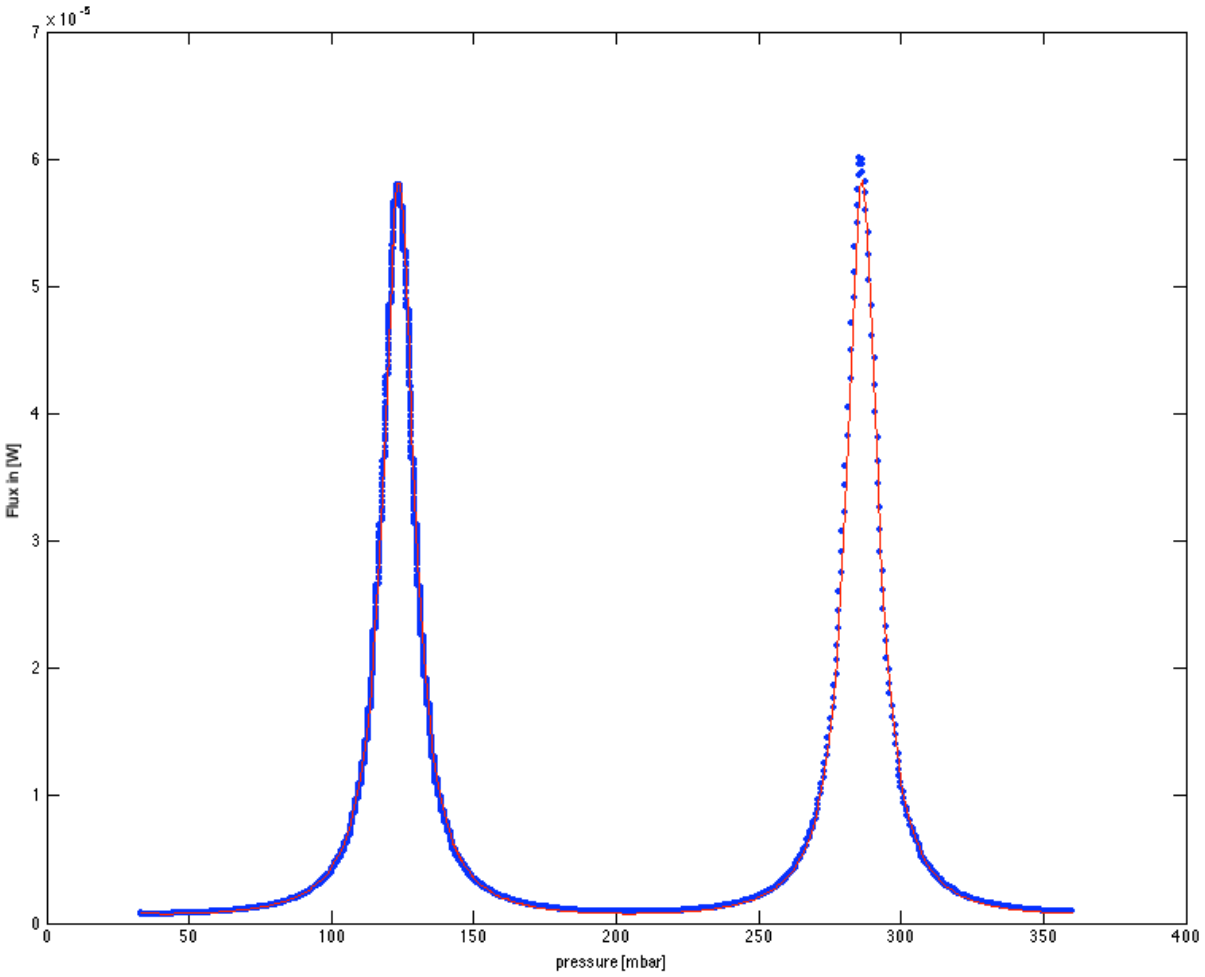

3.6 Etalon spacing

The etalon has been manufactured by ICOS to the designed gap of 7.6 mm within better than a fringe of the measuring interferometer, which is expected to be ***D* = 7.6 mm ± 0.0003 mm**. A final measurement will be done during system verifications of the ESPRESSO spectrograph by recording and fitting the entire FPC spectrum. By analogy with the HARPS FPC (see Section 3.13) we can however state that the gap *D* lies within **0.3 µm P-V** of the specified value.

3.7 Photon Noise

The ability of determining the position of a spectrum on the CCD (line position expressed in pixel) and associate it with a given wavelength depends on the width and the intensity of the line. In general one can say that the fundamentally attainable precision is proportional to the square root of the number of lines in the spectral domain and their intensity, and inversely proportional to their width. In HARPS, the formulae described by Bouchy & Pepe (2001) are employed to measure the fundamental (photon-noise limited) precision content of a spectrum.

Figure 4 shows the flux produced by the LDLS lamp within its the nominal 230 µm fiber illuminating the FPC. The emission is extremely flat and varies from 40 µW/nm to 50 µW/nm

from the red to the blue end od the spectral range of ESPRESSO. Let's assume the worst case, i.e. in the blue, where the photons 'weigh' more and the instrument transmittance is lower. At 380 nm we obtain a photon flux of about 10^{14} photons/s/nm out of the lamp fiber. Let's consider now a pessimistis PFC transmittance of 10%, a transmittance of the calibration unit of 50%, an étendue matching efficiency of 10%, and a spectrograph efficiency of 10%, we obtain a flux on the detector of the order of $5 \cdot 10^{10}$ ph s^{-1} nm^{-1}. The line width of a Fabry-Pérot line is given by its resolution $R_{FP} = F_E \cdot m = 12.3 \cdot 40'000 \approx 500'000$, where m is the order number of the FPC line at 380 nm. In nm, the linewidth is thus $w_{FP} = \lambda / R_{FP}$ =0.00076 nm. We expect therefore a photon flux of about $3.8 \cdot 10^7$ ph s^{-1} per spectral line of the FPC. From HARPS we can estimate that the RV precision delivered by a single line of about 10^6 photo-electrons is of the order of 1 m s^{-1}. By analogy we can therefore extrapolate that in an exposure of 10 seconds the RV-precision per line is of the order of 5 cm s^{-1} with the FPC of ESPRESSO. If we consider that the ESPRESSO spectrum contains of the order of 20'000 FPC lines, then we end up with a potential global precision of **0.04 cm s^{-1} in a 10-seconds exposure**, which means that we have a flux margin of the order of a factor 10'000 with respect to the specified requirement.

Figure 4: Flux of the LDLS lamp though-out the spectral range of ESPRESSO

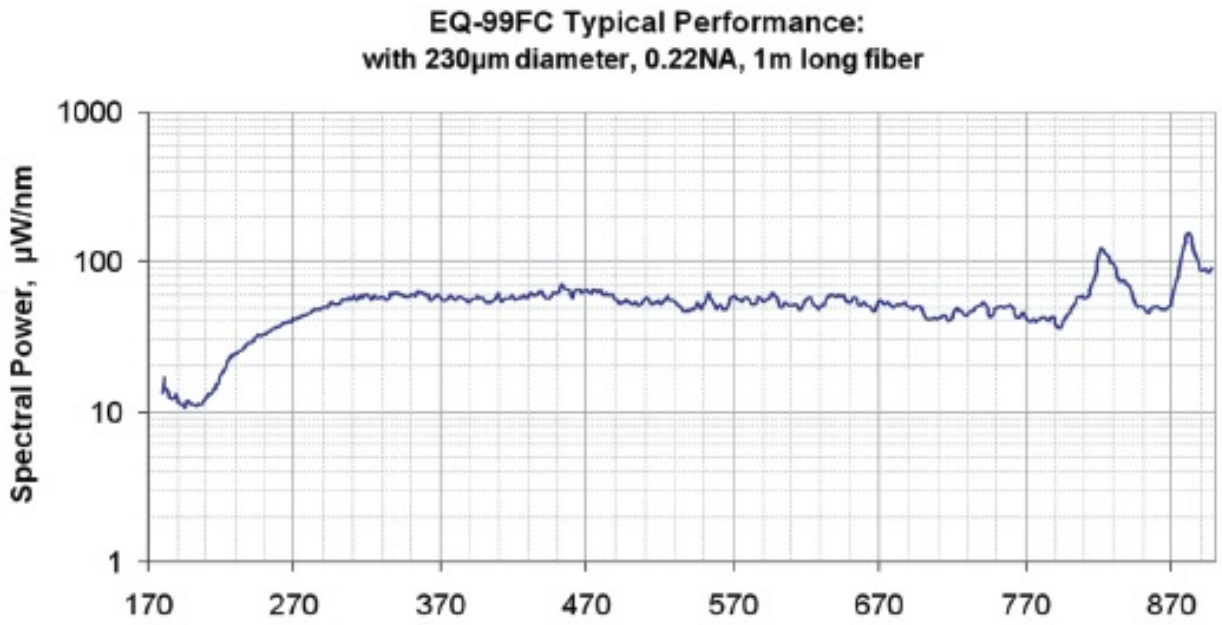

It is important to note that, in HARPS-N, we obtain 5 cm s^{-1} global RV precision in a 20-seconds exposure, after having attenuated the LDLS flux by a factor of 300. Figure 5 shows the attainable precision using the FPC system as a function of the square root of the relative flux measured on the detector. The flux was varied either by changing the variable ND-filter in front of the calibration lamp or by varying the exposure time. For comparison, also the results obtained with the hollow cathode thorium lamp are shown. In both cases it could be demonstrated that the relationship is perfectly linear as expected from pure photon noise, and that a precision of about 2 cm s^{-1} can be attained on a single spectrum.

Figure 5: Fundamental (photon-noise limited) precision obtained on a single FP spectrum. The results from the thorium lamp are shown for comparison.

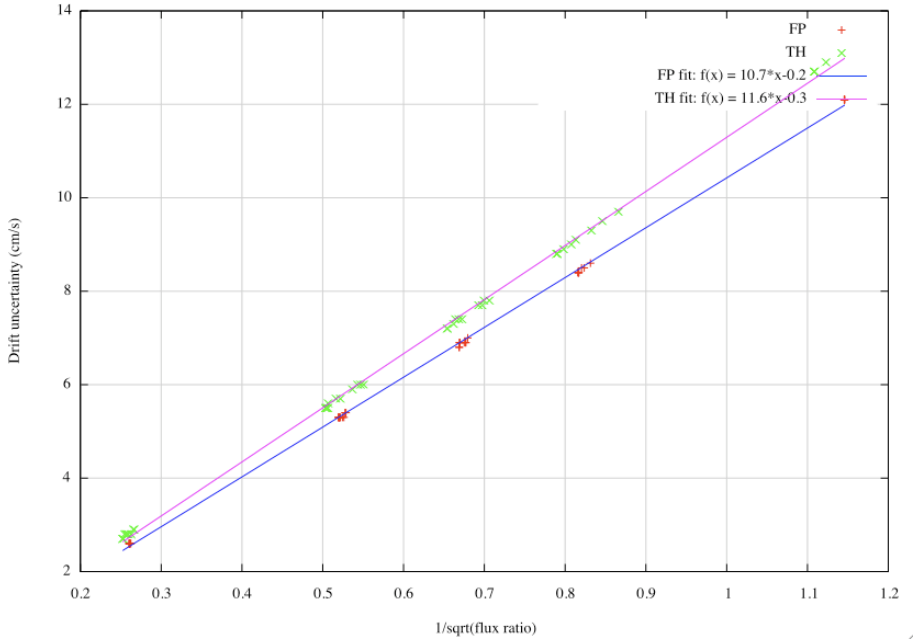

As mentioned above, the flux level can be varied either by increasing the light intensity or the exposure time. In the present HARPS-N system the thorium lamp is tuned in a way such to balance lifetime and flux. In an exposure of 20 s, which is the (minimum) nominal exposure time for a wavelength-calibration exposure, the attained precision level is of the order of 2 cm s^{-1}. Not only this directly demonstrated that the required photon-noise precision is achieved already with HARPS-N and a similar system, but also validated the performande theoretical computations, which are perfectly compliant with the HARPS-N measurement, if we consider that the coupling efficiency of the HARPS-N FPC has not been optimized in the same way as for ESPRESSO, and that the calibration and scientific fibers of HARPS-N are considerably longer that those of ESPRESSO.

In practice, and in order to not saturate the ESPRESSO detector, we will have to introduce fixed ND filter at the output of the lamp. The location is already foresee with the filter box between the LDLS lamp and the Vacuum Tank. The filter density will be adapted during system tests of ESPRESSO.

3.8 Flux Homogeneity

Given the flat spectral power of the LDLS and the flat spectral transmission of the FPC, the main driver for flux inhomogeneities is the energy of the photons across the spectrum. Since the photon energy increases by a factor of 2 from the red to the blue end of the spectral range, and that both the spectral power of the LDLS and the transmittance of the FPC both increase towards the blue, we do not expect flux inhomogeneities large than a factor of 2, thus perfectly with the specified maximum flux variation $\boldsymbol{F_{max}/F_{min} = 2 < 5}$.

3.9 Line Width

The line width of a Fabry-Pérot line is given by its resolution $R_{FP} = F_E \cdot m = 12.3 \cdot 40'000 \approx 500'000$, where m is the order number of the FPC line at 380 nm. The linewidth of the FPC is thus $w_{FP} = \lambda / R_{FP}$ =0.00076 nm. The size of the spectral element of ESPRESSO is given by the

spectral resolution R of the spectrograph, which is about $R = 140'000$ in its standard HR mode. Therefore, the width w_{SE} of the spectral element is $w_{SE} = \lambda/R$, which is about 0.0027 nm in the extreme blue and 0.0056 nm in the extreme red part of the spectrum. Therefore, in the worst case (blue), the FPC line width is $\boldsymbol{w_{FP} < 0.3 \cdot w_{SE}}$. The FPC is thus not only compliant with the line-width requirement for the HR mode, but also with the UHR mode of ESPRESSO. In no case the FPC lines are resolved by the spectrograph.

3.10 Line Separation

The line separation $\Delta\lambda$ of Fabry-Pérot lines is given by the formula $\Delta\lambda = \lambda^2/(2D)$. This value is minimum it the extreme blue, where it value is $\Delta\lambda_B = 0.00475$ nm and maximum in the red, where its value is $\Delta\lambda_R = 0.02$ nm. The ratio between the line separation and the width of the spectral element of ESPRESSO lies therefore between $\boldsymbol{\Delta\lambda_B/w_{SE} = 1.76}$ **and** $\boldsymbol{\Delta\lambda_R/w_{SE} = 7.4}$. Although these values are slightly non-compliant with respect to the specified values on boths ends, it must be noted, that it was already theoretically not possible to comply with them everywhere in the wide spectral range of ESPRESSO (more than a factor of 4 due to the spectral width!).

3.11 Short-Term Repeatability

The following sections are based on measurements and tests performed on the HARPS FPC, since the corresponding parameters can only be determined using a highly stably high-resolution spectrograph. The tests will be repeated for the ESPRESSO FPC one ESPRESSO is fully functional and stable.

In order to use the FPC in a standard way on HARPS, the DRS (pipeline) had to be adapted and some functionality added. In particular, one had to add the possibility of treating frames using the FPC on fiber B for both calibration and scientific (target) exposures. The recognition and the correct handling of the various cases had to be implemented. Also, for the measurement of the drift, several new algorithms have been tested and implemented.

It is important to note that these developments have been also used for the simultaneous development of the LFC by ESO and MPQ, since the LFC as well had to be tested on HARPS. The spectra of the LFC and the FPC are actually qualitatively identical, and the same data reduction can be used in both cases. These concepts have been fully integrated in the **ESPRESSO** pipeline and apply in an identical way for the Laser-Frequency Comb and the Fabry-Pérot.

We have tested the short-term stability by performing long series of ThAr-FP exposures (ThAr on fiber A, FPC on fiber B) and by computing the respective drifts independently. Figure 6 shows the drift from one exposure to the other as computed by the ThAr lamp and the FPC, as well as the difference of both to remove possible instrumental drifts.

For the ThAr alone we obtain a dispersion of about 0.19 m s^{-1} rms which should be compared to about 0.09 m s^{-1} pure photon-noise error. For the FPC we obtain 0.176 m s^{-1} rms dispersion, to be compared to 0.06 m s^{-1} photon noise. For the difference of both, we end up with a photon noise of 0.11 m s^{-1} and a measured dispersion of 0.14 m s^{-1}. The dispersion of the dirrence is well below the square root of the quadratic sum of the individual drift measurements of 0.26 m s^{-1}, demonstrating that both sources track a 'real' instrumental' drift. On the other hand, the difference between the photon noise and the measured dispersion leaves room for a 0.08 m s^{-1} additional dispersion, which is not 'seen' by at least one of the fibers (or better sources).

Figure 6: Relative drift measurements over 7 hours to test the short-term performances of the FPC

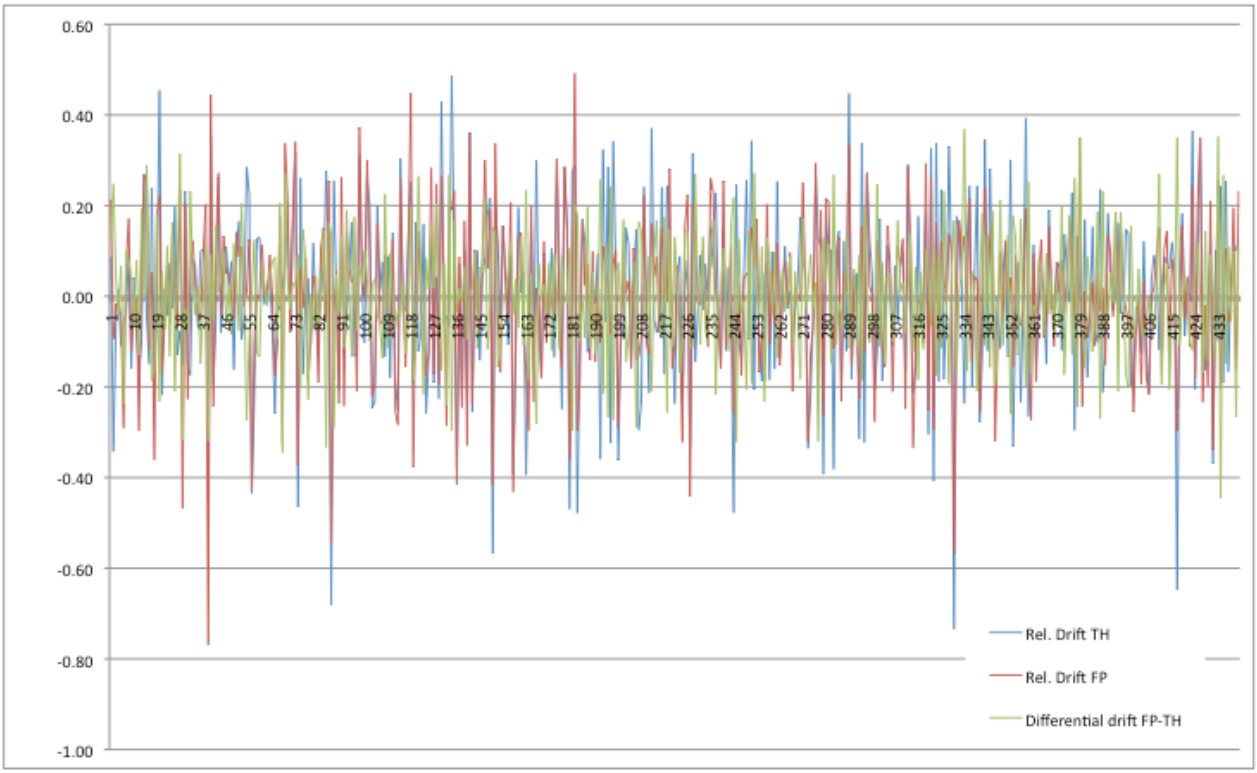

The plot in Figure 7 shows the same data, but this time in absolute terms, i.e. it indicates the absolute drift for FP and TH with respect to the very first exposure of the series. It should be remarked that in general the FP and the TH follow the same 'high-frequency' behavior, tracking real instrumental drifts. This is demonstrated by the fact that the dispersion of the difference is well below the dispersion of the individual measurements. On the other hand, the plot shows also that one can have differential drifts of the order of 0.9 m s^{-1} P-V or 0.23 m s^{-1} rms if no recalibration is performed during every night. Again, this is a worst case limit if we assume that the differential drift between TH and FP is fully due to the FP. As it will be demonstrated in the following, the short-term stability oft he FPC is well within specs.

Figure 7: Absolute drift measurements over 7 hours to test the short-term performances of the FPC

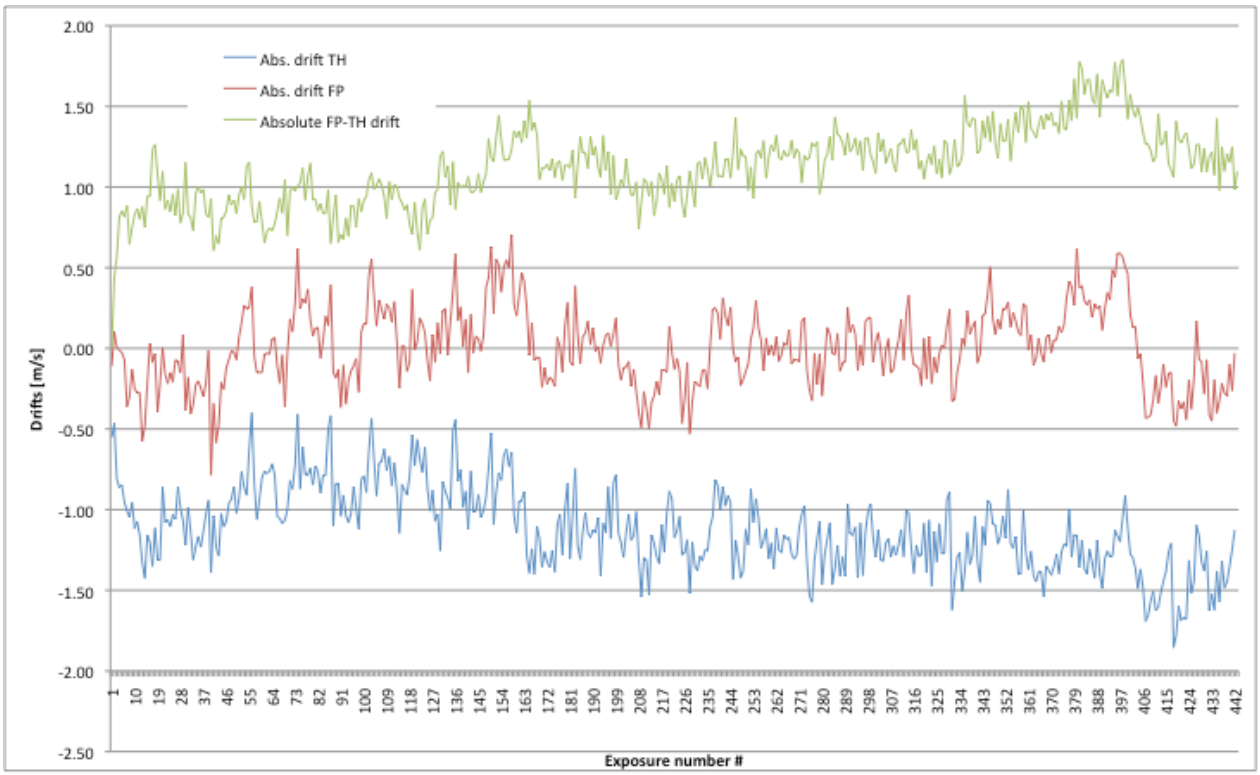

3.12 Long-Term Repeatability and Line-Shape Stability

The line-shape stability cannot be measured separately from the photocenter measurement and it is therefore measured as a part of the long-term repeatability. The long-term stability was tested in a similar way as the short-term stability using HARPS@ESO data. Frames were taken in routine operation almost every day. The idea was to monitor possible long-term drifts of the FPC with respect to the ThAr calibration lamp.

Figure 8 shows the results. Over the 6 months of operations in 2012, the FPC slowly drifted by a total of 11.6 m s^{-1}, assuming that the ThAr lamp has no internal drift. The measured drift is mostly due to the fact that the pressure in the FPC increases slightly with time, since it is not continuously pumped. This sequence shows nevertheless in a clear and impressive way that the long-term drift of the FPC is of about 0.063 m s^{-1} per day in average. During an observing night, between the calibration and the scientific exposures, we should not expect a drift larger than 0.05 m s^{-1}, if the daily calibrations are done at the beginning of the night.

Figure 8: Drift measurements over 180 days to test the long-term performances of the FPC

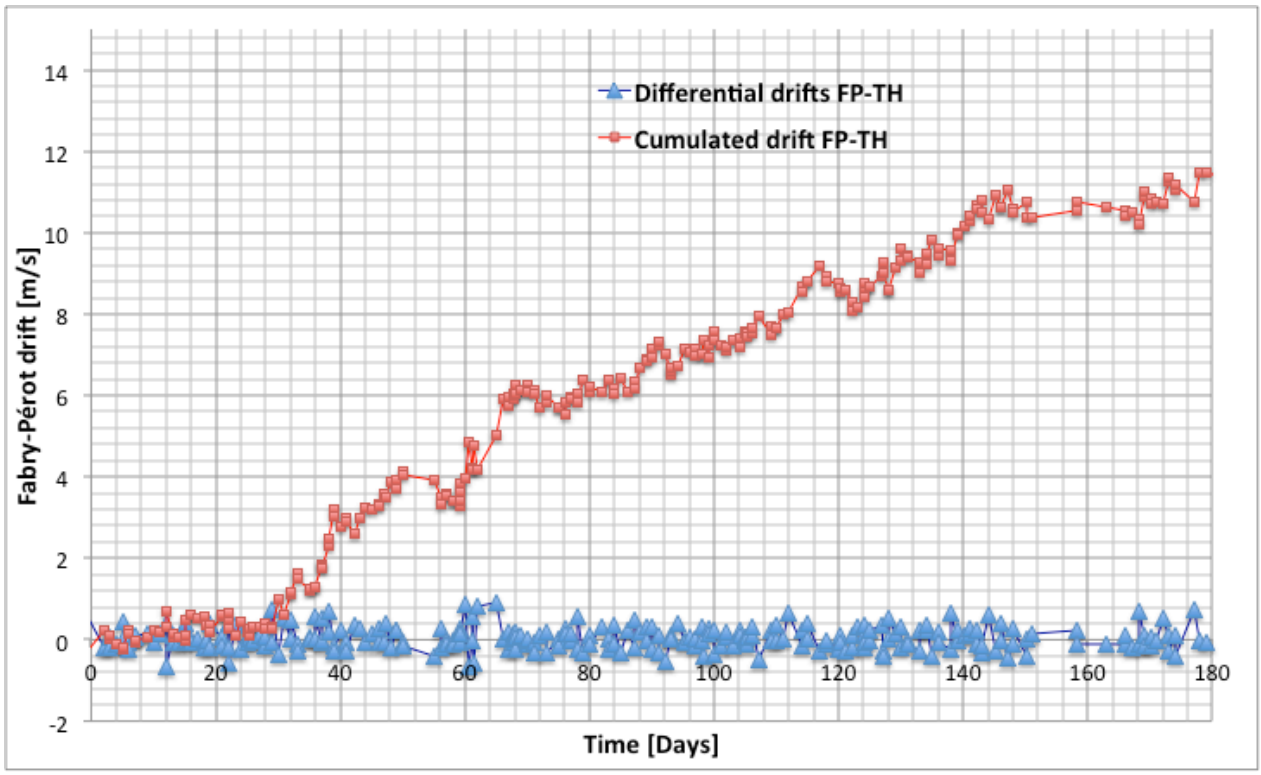

3.13 Local Wavelength Accuracy

For the theoretical Fabry-Pérot the wavelength (or frequency) of a given transmitted peak (order) m is fully determined by a single parameter: the gap D. The corresponding formula is $\lambda_m = 2D/m$. Provided that we know the etalon's gap, we can, from this formula, directly determine the wavelength of a given line by knowing it order number. In practice, however, one does not know the absolute order number of the line, but only a relative numbering by assuming that the peaks must have continuously increasing and discrete order values. We have therefore reversed the problem by using the spectrographs calibration delivered by the thorium source and used it to assign a wavelength to each transmission peak. Using this wavelength and assuming a gap of $2D$ = 14.6 mm for the FPC of HARPS, we have been able to determine directly the order number of each transmittance peak appearing in the FP spectrum.

We did not expect the gap D to be exactly the theoretical values, nor to be constant as a function of wavelength due to the varying effective optical depth of the dielectric mirror coatings. Indeed, the computed order numbers were not all perfectly discrete. Nevertheless, the difference to the discrete continuous number is always below 0.25. From this we can conclude that by rounding the obtained order number to the closest integer value we unambiguously identify the real order number. Using this fact, we have then used the so computed discrete order number and the wavelength assigned from the thorium calibration to determine the effective gap $D = D(\lambda)$ of the etalon. The result is shown in Figure 9. Note the mechanical gap of the etalon is of 7.3 mm and that in the figure the optical path difference $2D$ is actually shown.

Figure 9: Effective etalon gap $2D(\lambda)$ as a function of wavelength and is difference from the nominal value of 14.6 mm

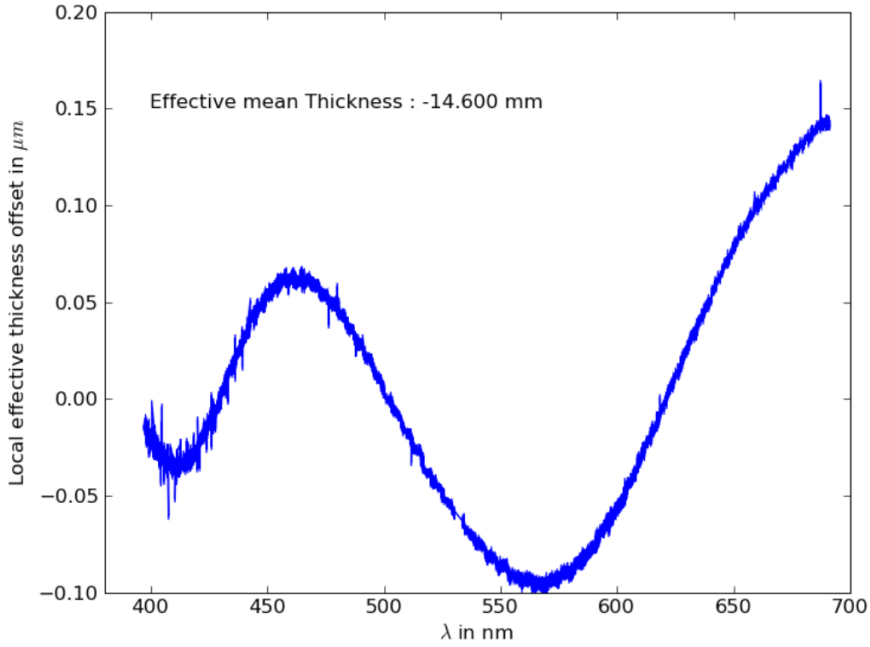

It appears that the 'manufactured' mechanical gap of D = 7.3 mm is fully compliant with the measured optical path difference of $2D$ = 14.6 mm within a quarter of wavelength, which confirms that the order numbering can be assigned unambiguously by assuming the theoretical gap value. If a wrong value D had been assumed, the $D(\lambda)$ would show a slope of at least one wavelength over the plotted spectral range.

Nevertheless, $D(\lambda)$ seems to vary significantly. The measured changes correspond to about 10^{-5} or, expressed in radial velocities, of the order of 3 km s^{-1}. We assume here that $D(\lambda)$ is constant in time and that thus the presented fact does not have any impact on ability of the FP system to track instrument drifts. However, we also conclude in order to use the FPC system for *absolute* wavelength calibrations to better that 10^{-5}, $D(\lambda)$ of the Fabry-Pérot must be calibrated by another mean (e.g. laser frequency comb or thorium lamp).

Although $D(\lambda)$ seems well determined we have to remark that short-scale patterns with amplitude of the order of 50 m s^{-1} have been recorded in $D(\lambda)$. At first glance the patters seems to be linked to the FP system itself (the pattern is the same when comparing wavelengths present in two different orders), and should be calibrated..

We conclude here that the FP etalon behaves as expected in terms of spectral performances. The etalon gap has been manufactured (and measured) with an amazing accuracy. We confirm that the effective gap $D(\lambda)$ varies with wavelength. However, we will see later that this gap $D(\lambda)$ remains constant with time and can be thus calibrated down to photon noise precision.

The effective etalon gap varies as a function of wavelength due to the fact that the penetration depth in the coating depends on the wavelength. By using the ThAr calibration of the FP frames. We have repeated this measurement in order to verify whether the etalon characteristic, in particular the coatings, remain constant with time. Figure 10shows the effective gap (twice the physical gap) as a function of wavelength. The two curves and the respective zoom show a measurement taken with the continuum laser source of HARPS in 2011 and another in 2012 more than one year later. Both plots show that the two curve follow each other to a large degree. The absolute variation of 0.3 µm corresponds to a 'velocity' of 6 km s^{-1}. The difference between the two curve is much smaller and basically an offset. It is mainly due to a pressure change in the

FPC system which influences the effective gap of the etalon. Small 'coherent' variations can be seen on short scale. They correspond to about 0.003 nm or 60 m s^{-1}.

Figure 10: Dispersion law of the FPC (expressed in effective etalon gap) recorded over two seasons separated by more than one year. Left: full wavelength range of HARPS. Right: Zoom over a single order.

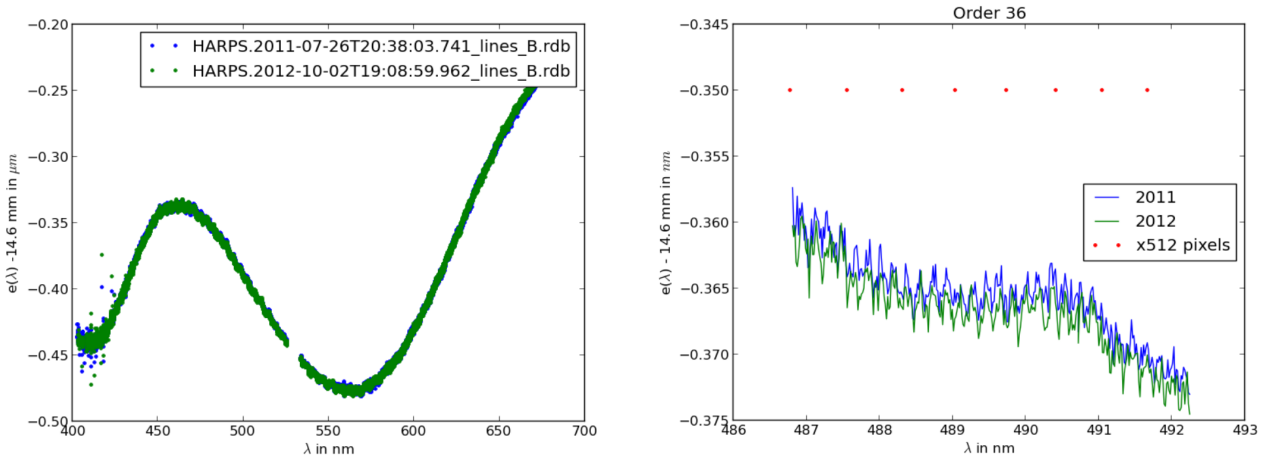

Figure 11shows the difference in dispersion between the two seasons separated by more than one year. The variation is expressed in terms of effective etalon gap variation. As it can be seen, the variation is constant with wavelength. The general offset of 0.65 nm (= 13.4 m s^{-1}) can be explained by the differences in pressure inside the etalon dewar between the two measurements. It interesting to note that the two curves show the same low-frequency behavior, confirming that the coatings characteristics remain unchanged to the level given by the measurement noise of each single line. It should be noted that the difference of the dispersions removes the 'coherent' wiggles seen in the absolute dispersion curve shown in the previous figure. The remaining difference of typical $\pm$1 nm or about $\pm$20 m s^{-1} is probably simply due to 'photon noise' when determining the line position on one single frame. Indeed, a back of the envelope estimation of the centroid error obtained on a line of 5000 electrons/extracted pixel, a typical value for the HARPS FPC frames, leads to an error of 20 m s^{-1}. On the HARPS-N FPC the flux is about a factor of 6 higher, such that we can expect that the FPC lines are determined with a precision of about 2.5 times better, i.e. to a typical precision of 8 m s^{-1}.

Figure 11: Dispersion variation (expressed in difference of effective etalon gap) between two seasons separated by one year as a function of wavelength. Left: full wavelength range of HARPS. Right: Zoom over a single order.

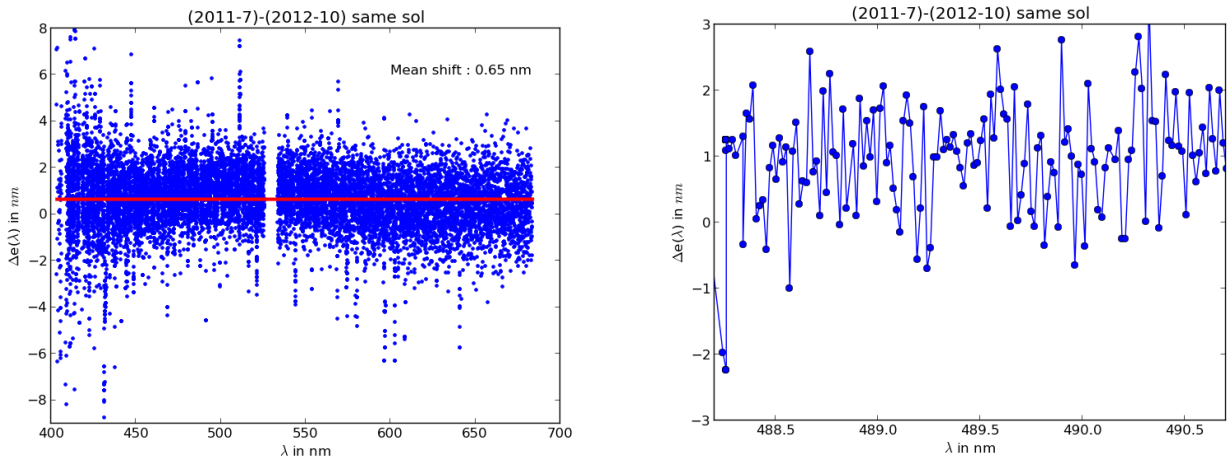

Chapter 4. Conclusions

We have described the exceptional performances of the ESPRESSO FPC and, together with the experience acquired on the HARPS FPC, we have demonstrated that the FPC is indeed a valuable fallback solution for the LFC under two aspects:

1. It is able to provide a drift measurement (simultaneous reference) well within the required photonic precision and short-term stability.
2. If combined with external absolute reference, it can be used to characterize the CCD and provide wavelength calibration. The global accuracy will be given by the external source. The local accuracy is given by the ability of calibration the group-delay dispersion of the Fabry-Pérot. Test on HARPS show that the dispersion law is reproducible within 1/30'000'000 of the Fabry-Pérot thickness, which corresponds to an equivalent local repeatability of 10 m s^{-1}.
3.